

# Overview of Ultrasonic Spinning Rheometry: Application to Complex Fluids

Taiki YOSHIDA<sup>\*,†</sup>, Yuji TASAKA<sup>\*\*</sup>, Kohei OHIE<sup>\*\*</sup> and Yuichi MURAI<sup>\*\*</sup>

<sup>\*</sup>National Institute of Advanced Industrial Science and Technology, Tsukuba Central 3, 1-1-1, Umezono, 305-8563 Tsukuba, Japan

<sup>\*\*</sup>Laboratory for Flow Control, Faculty of Engineering, Hokkaido University, N13W8, 060-8628 Sapporo, Japan

(Received: September 5, 2021)

A novel rheometry termed ultrasonic spinning rheometry (USR) is overviewed in this paper. This methodology utilizes ultrasonic velocity profiling as a representative velocimetry for various complex fluids including multi-phase state. The USR determines optimal properties from cost function which is calculated from both equation of motion and constitutive equation of test fluids by substituting the measured velocity profiles. Various examples are explained to indicate the applicability and efficacy of USR for measuring complex fluids; silicon oil, polymer solution, clay dispersion, water-oil two-phase fluid, and more. Through these results, we discussed future prospects of USR developments regarding its applicability and efficacy.

**Key Words:** Rheometry / Ultrasound / Velocity profiling / Viscoelasticity / Unsteady shear flow /

## 1. INTRODUCTION

Rotational/oscillatory shear rheometer is well-known as a representative means for rheological evaluation; the prototype has been completed more than a hundred years ago. For ensuring requisite assumptions of standard rheometer test, a narrow gap is usually set at measurement compartment. The assumptions for the rheometer, however, are not always satisfied due to the complex dynamics of non-Newtonian fluid, such as shear history effect,<sup>1)</sup> shear banding,<sup>2-4)</sup> wall-slip,<sup>5,6)</sup> elastic instability,<sup>7-9)</sup> and more. Furthermore, it is clearly observed that fluids with multi-phase dispersion cannot be measured due to jamming. From ten-odd years ago, the applicable range was extended by combining velocity profiling with a widened-gap rheometers.<sup>10)</sup> This improvement gives variable information to determine the actual shear strain rate under existence of shear localization. Rheological property based on both torque and modified shear strain, however, does not reflect the correct value, because the property has spatial gradient within the widened gap. Thus, a novel method for evaluating spatial distribution of rheological property is indispensable to overcome the limitation on conventional tools.

From the past decade, ultrasonic spinning rheometry (USR) has been progressively developed to overcome the problems of conventional tools. Using an open top cylindrical container, Sakurai *et al.* applied ultrasonic velocity profiling (UVP) to reveal the complex rheology of transient bubble deformations.<sup>11)</sup> Utilizing ultrasound gives a benefit confirming fluid dynamics in dispersion with opaqueness. Instead,

the original instantaneous velocity profile was substituted into equation of motion, so the noise was augmented due to differential calculation. Shiratori *et al.* visualized shear rate and strain field under unsteady flow<sup>12)</sup> and showed that it has the potential to be the pilot version of USR. In order to prevent noise augmentation, Tasaka *et al.* proposed an algorithm using phase-lag information of velocity profiles,<sup>13)</sup> where Fourier transform is applied to velocity distribution under periodic oscillatory shear flow; this is USR **Ver. 1.0**.

USR **Ver. 1.0** could evaluate local effective Newtonian viscosity by comparing the phase lag of the experimental result with the exact solution. In the process of measuring the effective Newtonian viscosity of various complex fluids, such as clay dispersion having thixotropic characteristic, liquid food gelling behaviors with tiny ingredients, and curry paste containing large ingredients,<sup>14)</sup> applicability of USR **Ver. 1.0** has advanced step by step. The macro-rheology in clay dispersion with both gel and sol are also discussed.<sup>15)</sup> As the property is approximated as locally effective Newtonian viscosity, USR **Ver. 1.0** still has room to explore the scope for improvement. Here, Tasaka *et al.* updated to USR **Ver. 2.0** which is viscoelasticity evaluation algorithm in a frequency domain.<sup>16)</sup> Basically, optimal properties are determined by substituting velocity profiles into the motion and constitutive equations. Completed by velocity measurement alone, multiple rheological properties can be evaluated without additional measurement. For enhancing the applicability and efficacy, USR continues to extend its function and algorithm by accumulating result of complex fluids.<sup>17-21)</sup>

In this overview, rheological properties of various fluids are evaluated with USR, and from the obtained results, we will

<sup>†</sup>Corresponding author.

E-mail: taiki.yoshida@aist.go.jp  
Tel: +81-29-861-8416

discuss the applicability and limitations of USR.

## 2. METHODOLOGY

We used open top acrylic cylinder with 2 mm thick walls, 145 mm inner diameter and 60 mm in height (Fig. 1a). A water bath surrounding the cylinder functions to propagate ultrasound inside the cylinder. The oscillation was controlled sinusoidally with angle  $\Theta$  and frequency  $f_0$ . The wall angular velocity is given as  $U_{\text{wall}} \sin(2\pi f_0 t)$ , where  $U_{\text{wall}} = 2\pi f_0 R\Theta$ . The UVP-DUO-MX (Met-Flow S.A., Switzerland) was used to measure instantaneous velocity distributions  $u_\xi(\xi, t)$ , where time and spatial resolutions are  $O(10 \text{ ms})$  and  $O(0.1 \text{ mm})$ . Mounted with a distance of  $\Delta y$  from the cylinder center, the azimuthal velocity component is obtained by an ultrasonic transducer (resonance frequency 4 MHz and 5 mm active element diameter). The ultrasonic pulse is emitted having a disk-like volume for measuring velocity (Fig. 1b). Assuming axisymmetric flow, the azimuthal velocity  $u$  is calculated from a geometric relation given as  $u = u_\xi r / \Delta y$ , where  $\Delta y = 15 \text{ mm}$  is suitable for propagating ultrasonic pulse beam inside the cylinder.

For 500 cSt silicon oil, the instantaneous velocity profiles under oscillation frequency  $f_0 = 0.5 \text{ Hz}$  are shown in Fig. 1(c) as a radial-temporal distribution, where the dashed curve indicates the trend of phase difference from the cylinder wall. With time, the velocity fluctuations were propagated from the cylinder wall ( $r/R = 1$ ) to the interior. USR evaluates rheological property by utilizing phase lag information,

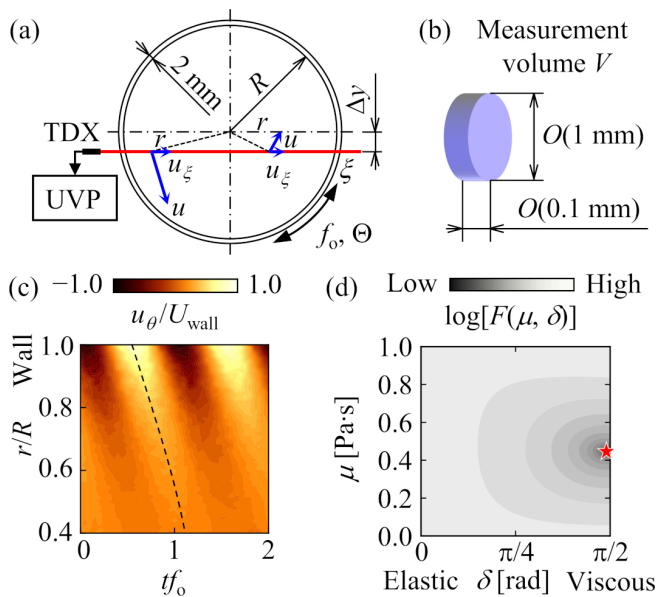


Fig. 1 Schematics of (a) top view of acrylic cylindrical container for fluid velocity measurement, (b) apparent measurement volume considered from ultrasonic pulse, (c) azimuthal velocity distribution of silicone oil (0.49 Pa·s) with  $f_0 = 0.5 \text{ Hz}$ , and (d) cost function distribution  $F(\mu, \delta)$  at  $r/R \approx 0.9$  in (c).

characterized by a specific property satisfying the equation of motion, spatially and temporally.

In the USR algorithm, there are broadly two ways, USR **Ver. 1.0** and **2.0**, to evaluate rheological properties. In this overview, we focus on the algorithm of USR **Ver. 2.0** which is described in the following. Assuming that fluid flows are one-directional and axisymmetric, Cauchy's equation of motion is given as  $\rho \partial u / \partial t = (\partial / \partial r + 2/r)\tau$ , where  $\rho$ ,  $\tau$ , and  $u$  indicate fluid density, shear stress, and flow velocity. To describe the relation of  $u$  and  $\tau$ , a constitutive equation,  $\tau = f(\dot{\gamma}, \Pi_1, \Pi_2, \Pi_3, \dots)$  is required, where  $\dot{\gamma}$  is shear strain rate, given as  $(\partial / \partial r - 1/r)u$ , and  $\Pi$  represents a series of rheological indexes. For instance, the Maxwell model is the simplest expression for linear viscoelasticity, written as  $\tau + (\mu/E)\partial\tau/\partial t = \mu(\partial u/\partial r - u/r)$ , where  $\mu$  and  $E$  indicate the viscosity and elasticity.

From Fourier transform with respect to  $t$ , Cauchy's equation and the Maxwell model can be modified as  $i\omega\rho\hat{u} = (\partial/\partial r + 2/r)\hat{\tau}$  and  $\hat{\tau} + i\omega(\mu/E)\hat{\tau} = \mu(\partial/\partial r - 1/r)\hat{u}$ , where the Fourier-transformed velocity and shear stress are denoted as  $\hat{u}(r, \omega) = \mathcal{F}[u(r, t)]$  and  $\hat{\tau}(r, \omega) = \mathcal{F}[\tau(r, t)]$ , with the angular frequency  $\omega$ . Here  $\delta$  is defined as  $\tan \delta = E/\omega_0\mu$  which is an indicator showing phase difference between viscous and elastic. Intermediate values of  $\delta$  indicate viscoelastic behavior. Considering the cost function,

$$F(\mu, \delta; r)|_{\omega=\omega_0} = \left| i\omega\rho\hat{u} - \left( \frac{\partial}{\partial r} + \frac{2}{r} \right) \hat{\tau} \right|, \quad \text{s.t. } \hat{\tau} + i \frac{1}{\tan \delta} \hat{\tau} = \mu \left( \frac{\partial}{\partial r} - \frac{1}{r} \right) \hat{u}, \quad (1)$$

$\mu$  and  $\delta$  can be determined by satisfying the optimization problem with minimizing the cost function  $F$ . Fig. 1(d) shows the cost function  $F(\mu, \delta)$  at  $r/R \approx 0.9$  with substituting the velocity of Fig. 1(c) into Eq. (1). The minimal point of  $F$  shown by star plot is an optimal solution of  $\mu$  and  $\delta$ , where the  $\mu$  accords with catalog value, and the  $\delta$  indicates pure viscous characteristic. The effective shear stress and strain rate can be obtained by substituting the Fourier components of the measured velocity into the equation,  $\dot{\gamma}_{\text{eff}} = |(\partial/\partial r - 1/r)\hat{u}|$ ,  $\tau_{\text{eff}} = \mu \sin^2 \delta |1 - i/\tan \delta| (\partial/\partial r - 1/r)\hat{u}$ , where  $\mu$  and  $\delta$  are determined by solving the optimization problem in Eq. (1).

## 3. APPLICATIONS

The determined properties of  $\mu(\dot{\gamma})$  and  $\delta(\dot{\gamma})$  are shown in Figs. 2(a) and 2(b). As a typical Newtonian fluid, **silicon oil** was measured to ensure efficacy of USR.<sup>17)</sup> The blue colored plots in Fig. 2(a) show the result with viscosity  $\mu = 0.97 \text{ Pa}\cdot\text{s}$

(catalog value) which was close to the ideal value in a wide range of shear rate. In the horizontal axis, shear rate  $\dot{\gamma}$  is given with the range from  $O(10^0 \text{ s}^{-1})$  to  $O(10^1 \text{ s}^{-1})$ . The maximum and minimum values of  $\dot{\gamma}$  are determined by  $U_{\text{wall}}$  and limited by the performance of velocity profiling system. As examples showing shear thinning viscosity and viscoelasticity, the properties of **polymer solutions** (carboxymethyl cellulose; CMC and polyacrylamide; PAM) were also evaluated<sup>17,19</sup> as shown with pink colored and cross plots in Fig. 2, respectively. Here, the results of polymer solutions were drastically different compared to results obtained from the silicon oil; the  $\mu$  decreases with increasing  $\dot{\gamma}$ , and the  $\delta$  indicates proximity of being viscoelastic. As an example for a more complex fluid showing thixotropic characteristics, **clay dispersion** (montmorillonite) was evaluated. The results of clay dispersion are shown in gray plots and its thixotropy is caused by the interaction between dispersed particles.<sup>15,17</sup> The  $\mu$  drastically changes at the interface of gel and sol, where the interface is indicated as star shaped plot and determined by the phase lag profile.<sup>18</sup> The spatial evaluation mentioned above is an emphasized advantage of USR in comparison with standard rheometer which often shows heterogeneity due to shear history effect.

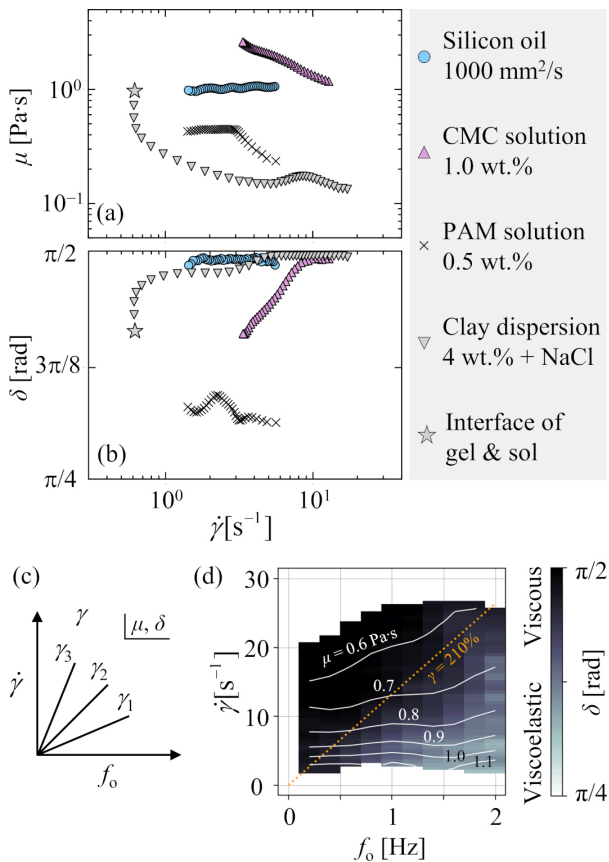


Fig. 2 The rheological properties (a)  $\mu(\dot{\gamma})$  and (b)  $\delta(\dot{\gamma})$  in some fluids with oscillation frequency  $f_0 = 0.5 \text{ Hz}$ , and application of rheology mapping; (c) schema and (d) example of CMC solution with 1.0 wt.%.

The oscillation frequency in the results shown in Figs. 2(a) and 2(b) was fixed at  $f_0 = 0.5 \text{ Hz}$ . Since the properties, of course, vary depending on the applied oscillation frequency, a representation termed “rheology mapping” has been recently introduced to evaluate the dependence of viscoelasticity on both deformation and timescale of the applied oscillatory shear.<sup>21</sup> As shown in Fig. 2(c), the characteristic such as being viscous or viscoelastic is clarified by multi-variable factors, where the example of application to CMC solution 1.0 wt.% is shown in Fig. 2(d).

As an example of USR application to multi-phase fluids, rheological property of **water-oil two-phase fluid** was evaluated.<sup>20</sup> This work examines the change in viscosity with time caused by the separation of water and oil mixture from difference in density. Small water droplets having  $O(0.1 \text{ mm})$  to  $O(1.0 \text{ mm})$  with a mean diameter were uniformly dispersed in thick silicon oil ( $1000 \text{ mm}^2/\text{s}$ ), and the volume fraction on the measurement line of UVP decreased with time. After evaluating  $\mu(\dot{\gamma})$  in each time, time variation of power law fitting parameters,  $n$  and  $K$ , was calculated to understand the effects of volume fraction and shear rate (Fig. 3). With time,  $n$  increases from 0.9 toward 1.0 and  $K$  decreases from 1.5 times the catalog viscosity toward the same value. As a notable conclusion, the evaluated viscosity was larger than the theoretical value because an increase of effective volume fraction or non-equilibrium deformation of the droplets increased viscosity.

As another example of USR application, **air-oil two-phase fluid** was examined; viscoelasticity of bubbles deforming under oscillatory shear is evaluated.<sup>16</sup> Applying linear viscoelastic analysis, separation of influences of unsteady bubble deformation into viscous and elastic contributions on the momentum propagation is achieved. Calculated at each radial position from  $r/R = 0.6$  to 0.95, the viscoelasticity evalua-

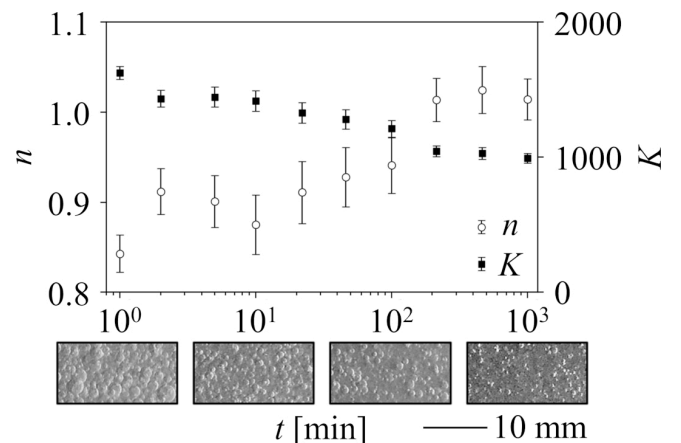


Fig. 3 Time variation of power law fitting parameters  $n$  and  $K$ , where error bars represent standard deviation.

tions of bubble dispersion are summarized in Table I. Here,  $\delta$  takes  $90^\circ$  without a region  $r/R \geq 0.9$ , and the elastic contribution appears in the region. The obtained results are reasonable considering that the capillary number exceeds the critical to allow bubble deformations in this range. The bubbles under oscillatory shear flow are deformed and restored periodically due to strong shear and relaxation. So, the elastic effect may be provided by restoring the original spherical shape in the relaxation.

Further, as an example elucidating physics of fluids, **polymer solutions with dispersed spherical particles** were examined.<sup>19)</sup> The particles dispersed in viscoelastic fluid are aligned in shear direction under unsteady flow/deformation (Fig. 4a). Significant result showing particle alignment has seldom been indicated in previous research using experimental approaches. By means of USR, the effective viscosity with particle alignment was evaluated as a much thinner viscosity estimated by Newton's law of viscosity (Fig. 4b), and the effective elasticity was estimated with a value augmented depending on volume fraction of particles (Fig. 4c). In this study, it is concluded that particle alignments modulate the effective viscoelasticity and the aligning particles are closely related to the relaxation time of fluid media. This is representative time scale of viscoelastic fluid with deformations.

To contribute to promoting quality of life, food rheology regarding texture evaluation has been recently started. A **gel made of low methoxyl pectin** was evaluated as a test food which is used as a thickener for medical purpose.<sup>18)</sup> For example, Fruiche (House Foods Group, Inc., Japan) is a representative commercial dessert in Japan, shown in Fig. 5. The Fruiche displays highly complex-rheological properties such as shear thinning viscosity, viscoelasticity, yield stress, thixotropy, and modifications of the effective viscosity by formless multi-phase dispersion. Fig. 5 shows that the effective viscosity of Fruiche decreases and converges to certain profile overall  $\dot{\gamma}$ , with increasing oscillation cycles. This evaluation has been considered as an improbable task as shear history effects

Table I Evaluation results of air-oil bubble suspension under oscillatory shear flow with  $f_0 = 1.0$  Hz; shear rate  $\dot{\gamma}$ , viscosity  $\mu$ , elasticity  $E$ , and phase difference in linear viscoelasticity  $\delta$  at different radial position  $r/R$ .<sup>16)</sup>

$r/R$	$\dot{\gamma}(\text{s}^{-1})$	$\mu(\text{Pa}\cdot\text{s})$	$E(\text{Pa})$	$\delta(^{\circ})$
0.95	15.89	1.46	39.8	77.1
0.9	14.28	1.32	121.2	86.1
0.85	12.46	1.17	–	90.0
0.8	10.53	1.05	–	90.0
0.75	8.63	0.99	–	90.0
0.7	6.90	0.97	–	90.0
0.65	5.45	0.99	–	90.0
0.6	4.32	1.05	–	90.0

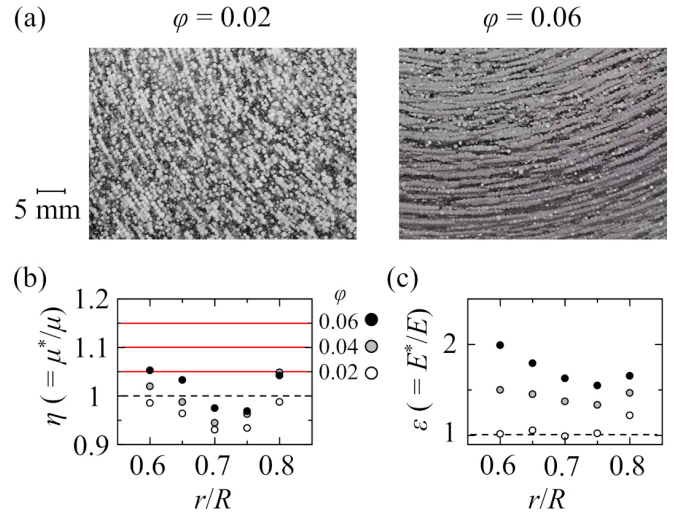


Fig. 4 (a) Photograph taken from the top of cylinder under room lighting in the PAM solution during oscillations, (b) radial profile of relative viscosities  $\eta$ , where the solid line indicates that estimated by  $\eta = 1 + 5\varphi/2$ , and (d) radial profiles of relative elasticities  $\epsilon$ .

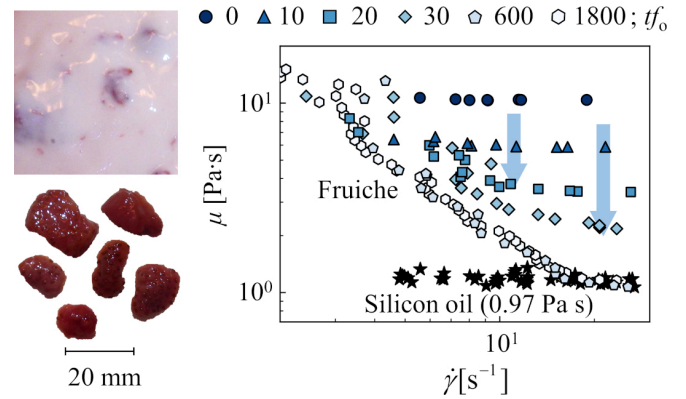


Fig. 5 Photographs of Fruiche and its ingredients, and  $\mu(\dot{\gamma})$  profiles with increasing oscillation cycle, where  $f_0 = 1.0$  Hz.

cannot be ignored in tests done by standard rheometers.

## 4. SUMMARY & PROSPECT

Through a series of applications to various complex fluids, ultrasonic spinning rheometry (USR) has been developed to extend its applicability and efficacy. The present overview of USR highlighted following applications in which advantages of USR are maximized; (1) test fluids which have the concern of being influenced by shear history effects as it is in standard rheometers, (2) fluids with co-existence of gel and sol, (3) fluid with multi-phase dispersion, (4) fluid with transient change in rheological properties (*e.g.* chemical reaction).

Further updates toward USR **Ver. 3.0** are progressing in two aspects. One is to realize a novel measurement system for pipelines, which will enhance the velocity profiling rheometry techniques in industrial usage. This methodology has

already been developed and has succeeded in evaluating rheological property of fluids inside a steel pipe from the outside by measuring velocity profiles. Hence, this method enables non-intrusive evaluations of flowing fluids inside pipes.<sup>22)</sup> The other is to improve and optimize ultrasonic velocity profiling for USR. Due to hardware limitations of velocity profiling, measurable ranges in shear rate and oscillation frequency are limited in  $O(10^0 \text{ s}^{-1})$  to  $O(10^1 \text{ s}^{-1})$  and  $O(10^{-1} \text{ Hz})$  to  $O(10^0 \text{ Hz})$  for the current USR. Radical improvement of measuring velocity will make a breakthrough in discovering unexplored issues on complex fluid rheology.

## ACKNOWLEDGMENTS

The authors express their gratitude to Dr. Peter Fischer, Dr. Erich J. Windhab, ETH Zürich, Switzerland, and Dr. Atsuko Namiki, Nagoya University, Japan for fruitful discussion, assistance, and cooperation in research and development.

## REFERENCES

- 1) Wolthers W, Duits MHG, van den Ende D, Mellema J, *J Rheol*, **40**, 799 (1996).
- 2) Fischer P, Wheeler EK, Fuller GG, *Rheol Acta*, **41**, 35 (2002).
- 3) Divoux T, Fardin MA, Manneville S, Lerouge S, *Annu Rev Fluid Mech*, **48**, 81 (2016).
- 4) Ito M, Yoshitake Y, Takahashi T, *J Rheol*, **60**, 1019 (2016).
- 5) Nechyporchuk O, Belgacem MN, Pignon F, *Carbohydr Polym*, **112**, 432 (2014).
- 6) Yang K, Yu W, *J Rheol*, **61**, 627 (2017).
- 7) McKinley GH, Byars JA, Brown RA, Armstrong RC, *J Non-Newtonian Fluid Mech*, **40**, 201 (1991).
- 8) Gallot T, Perge C, Grenard V, Fardin MA, Taberlet N, Manneville S, *Rev Sci Instrum*, **84**, 045107 (2013).
- 9) Fardin MA, Perge C, Casanellas L, Hollis T, Taberlet N, Ortín J, Lerouge S, Manneville S, *Rheol Acta*, **53**, 885 (2014).
- 10) Derakhshandeh B, Vlassopoulos D, Hatzikiriakos SG, *Rheol Acta*, **51**, 201 (2012).
- 11) Sakurai K, Tasaka Y, Murai Y, *Trans JSME Ser B (in Japanese)*, **79**, 1 (2013).
- 12) Shiratori T, Tasaka Y, Murai Y, Takeda Y, *J Vis*, **16**, 275 (2013).
- 13) Tasaka Y, Kimura T, Murai Y, *Exp Fluids*, **56**, 1867 (2015).
- 14) Yoshida T, Tasaka Y, Murai Y, *J Rheol*, **61**, 537 (2017).
- 15) Yoshida T, Tasaka Y, Tanaka S, Park HJ, Murai Y, *Appl Clay Sci*, **161**, 513 (2018).
- 16) Tasaka Y, Yoshida T, Rapberger R, Murai Y, *Rheol Acta*, **57**, 229 (2018).
- 17) Yoshida T, Tasaka Y, Murai Y, *J Rheol*, **63**, 503 (2019).
- 18) Yoshida T, Tasaka Y, Fischer P, *Phys Fluids*, **31**, 113101 (2019).
- 19) Yoshida T, Tasaka Y, Murai Y, *Phys Fluids*, **31**, 103304 (2019).
- 20) Ohie K, Yoshida T, Park HJ, Tasaka Y, Murai Y, *Trans JSME (in Japanese)*, **86**, 20-00242 (2020).
- 21) Ohie K, Yoshida T, Tasaka Y, Sugihara-Seki M, Murai Y, *Proc of 13<sup>th</sup> ISUD*, (2021).
- 22) Tasaka Y, Yoshida T, Murai Y, *Ind Eng Chem Res*, **60**, 11535 (2021).